Low-Temperature Kinetics of the Charge- and Atom-Transfer Reactions (Br^+, HBr^+ [$^2\Pi_i$, v^+], DBr^+ [$^2\Pi_i$, v^+]) + (HBr, DBr) → (HBr^+, DBr^+, H_2Br^+, D_2Br^+, $HDBr^+$)

Andrey E. Belikov† and Mark A. Smith*

Department of Chemistry, University of Arizona, Tucson, Arizona 85721

Received: November 18, 2003; In Final Form: January 29, 2004

The charge- and atom-transfer reactions between Br^+, HBr^+, and DBr^+ ions and HBr and DBr molecules have been studied in a HBr + DBr + He free jet. The ionic reactants in specific internal states were prepared by resonance multiphoton ionization of either HBr or DBr, and the ionic products were analyzed by mass spectrometry. A set of eight energetically possible reactions was considered in each case, including ions born in near-resonant ionization and photodissociation processes. Kinetic equations were integrated numerically over the appropriate reaction time and an optimization problem was solved to determine rate coefficients fit to final fractions of all ions measured in an experiment. Analytical expressions for the final fractions also were obtained and were used to derive the rate coefficients more accurately. The work is an example of a multireaction study without direct observation of all the reaction products.

I. Introduction

In our previous studies,[1,2] we have investigated the state-selective hydrogen and deuterium atom-transfer reactions

$$HBr^+ [^2\Pi_i, v^+] + H_2 \rightarrow H_2Br^+ + H \quad (1a)$$

$$HBr^+ [^2\Pi_i, v^+] + HBr \rightarrow H_2Br^+ + Br \quad (2a)$$

and

$$DBr^+ [^2\Pi_i, v^+] + D_2 \rightarrow D_2Br^+ + (D) \quad (1b)$$

$$DBr^+ [^2\Pi_i, v^+] + DBr \rightarrow D_2Br^+ + Br \quad (2b)$$

for the ($i = {}^1/_2, {}^3/_2$; $v^+ = 0, 1$) internal states of the ions. The rate coefficients of reactions 1 demonstrated clear threshold behavior and reached values of $\sim 2 \times 10^{-11}$ cm^3/s for the highest studied states of the ions. At the same time, rates of the highly exothermic reactions 2 were almost 2 orders of magnitude faster ($\sim 1.3 \times 10^{-9}$ cm^3/s) and had to be taken into account, even at a very low fraction of bromide molecules in the reacting mixture.

Information about charge- and atom-transfer reactions between hydrogen (deuterium) bromide ions and parent molecules (or their isotope equivalents) is rather limited. Green et al.[3] studied possible channels of the thermal reaction of the HBr^+ ions with HBr and DBr molecules and found the total rate coefficients to be 6.9×10^{-10} cm^3/s and 5.8×10^{-10} cm^3/s, respectively, inclusive for charge-transfer (46% and 50% for HBr and DBr), proton-transfer (32% and 28%), and atom-transfer (22% for both) channels. Low-temperature rates of these reactions seemed to be faster by a factor of ~ 2.[1,2] The negative temperature dependence might be easily explained if the reaction proceeded through the formation of collisional complexes[4−8] or simply through the attractive ion−dipole interaction potential. According to the estimations of Green et al.,[3] a complex mechanism was realized in ~30% of the reaction events under thermal conditions.

The state-selective charge-transfer reaction

$$DBr^+ (^2\Pi_i, v^+) + HBr \rightarrow HBr^+ (^2\Pi_{i'}, v'^+) + DBr \quad (3)$$

was investigated by Xie and Zare,[9] under thermal conditions, for $i = {}^1/_2, {}^3/_2$; $v^+ = 0, 1$. The rate coefficients summed over all energetically permitted states of products were determined to be 4.1×10^{-10}, 1.4×10^{-10}, 3.8×10^{-10}, and 2.3×10^{-10} cm^3/s for the ($^3/_2$, 0), ($^3/_2$, 1), ($^1/_2$, 0), ($^1/_2$, 1) states of the reactant. A similar tendency toward lower rate coefficients with vibrational excitation was observed[2] for reactions 2 with DBr^+.

Presently, we report the results of a more-detailed study of all possible ion−molecule reactions in the HBr + DBr mixture after state-selective (2+1) resonance-enhanced multiphoton ionization (REMPI) of either HBr or DBr molecules. When the (2+1) REMPI of HBr (DBr) is explored in the HBr + DBr mixture, some fraction of minor ionic species (DBr^+ (HBr^+) and Br^+) is always present. The first are born in near-resonance ionization processes (or in resonance if the resolution of the ionizing laser is low), because of similar internal states; the second are presumably products of the photodissociation of the HBr^+ and DBr^+ ions. These minor ions were included in the kinetic consideration, because they can have a significant role in the production of common product ions. In Section II, we describe the experimental technique for a kinetic study of the ion−molecule reactions in the free jet flow reactor based on the REMPI preparation of reactants and mass spectrometry of the products. The set of kinetic equations for ion−molecule reactions in a free jet is presented in Section III, both in its general form and in application to the reactions in the (HBr + DBr + HBr^+ + DBr^+ + Br^+) mixture. The rate coefficients have been found using two procedures. The first one, described in Section IV, is the numerical simulation of the reactions in the free jet and fitting to the experimental data. This simulation provides preliminary values of the rate coefficients and, what may be more important, gives the opportunity to analyze the role of every reaction in determining the final distribution of

* Author to whom correspondence should be addressed. E-mail: msmith@u.arizona.edu.

† Present address: Institute of Thermophysics, 1, Lavrentjev Ave., Novosibirsk, 630090, Russia.

10.1021/jp031254k CCC: $27.50
Published on Web 03/18/2004

TABLE 1: Reactions in the (HBr + DBr) Mixture after Photo-ionization of the Bromide Ions HBr^+, DBr^+, and Br^+, and Their Rate Coefficients

			Rate Coefficient (10^{-9} cm^3/s)[b]				
	reaction	$\Delta_f H$[a] (kcal/mol)	$f\,^3\Delta_2$ (v = 0)	$f\,^3\Delta_2$ (v = 1)	$F\,^1\Delta_2$ (v = 0)	$F\,^1\Delta_2$ (v = 1)	accuracy (%)[b]
R1[c]	$HBr^+ + HBr \rightarrow H_2Br^+ + Br$	-8.8 ± 0.5	1.3 [1.5]	1.0 [1.0]	1.3 [1.4]	1.1 [1.0]	20 [30]
R2	$HBr^+ + DBr \rightarrow HDBr^+ + Br$	-8.8 ± 1	1.7 [1.6]	1.7 [1.6]	1.6 [1.6]	1.6 [1.6]	20 [35]
R3	$HBr^+ + DBr \rightarrow DBr^+ + HBr$	$+0.5 \pm 0.5$		0.6[d] [0.6] for all ionization schemes			[100]
R4[e]	$DBr^+ + DBr \rightarrow D_2Br^+ + Br$	-8.7 ± 1	1.4 [1.5]	1.1 [1.1]	1.4 [1.4]	1.1 [0.9]	17 [30]
R5	$DBr^+ + HBr \rightarrow HDBr^+ + Br$	-9.7 ± 1	1.6 [1.6]	1.7 [1.6]	1.5 [1.6]	1.5 [1.6]	20 [35]
R6[f]	$DBr^+ + HBr \rightarrow HBr^+ + DBr$	-0.5 ± 0.5		0.6 [0.6] for all ionization schemes			50 [100]
R7	$Br^+ + HBr \rightarrow HBr^+ + Br$	-3.4 ± 0.5	2.7 [2.5]	2.7 [2.5]	2.8 [2.5]	2.6 [2.5]	14 [30]
R8	$Br^+ + DBr \rightarrow DBr^+ + Br$	-2.4 ± 0.5	1.6 [1.8]	1.6 [2.5]	1.7 [2.5]	1.6 [2.5]	18 [35]

[a] Based on Lias et al.[12] (see text in Section III). [b] Results of numerical simulation given in square brackets. [c] Data for thermal conditions from Green et al.: $k_1 = 0.7 \pm 0.2$;[3] low-temperature data from Belikov et al.: $k_1 = 1.4 \pm 0.2$.[1,2] [d] Assumed to be equal to k_6. [e] Low-temperature data from Belikov et al.: $k_4 = 1.3 \pm 0.3$.[1,2] [f] Data for thermal conditions from Xie and Zare: $k_6 = 0.4 \pm 0.08$.[9]

products. Analytical expressions for the final ionic distribution, as a function of experimental parameters, are obtained in Section V and applied to the derivation of the rate coefficients in Section VI that have been discussed in Section VII.

II. Experiment

Kinetics of the ion−molecule reactions were studied in a free jet flow reactor, using (2+1) REMPI for preparation of the ionic reactants and time-of-flight (TOF) mass spectrometry for analysis of the ionic products. The experimental equipment and techniques have been described in detail elsewhere;[10] thus, here we discuss only the salient features. A pulsed axisymmetric nozzle (General Valve) with an orifice diameter of 0.4 mm was used as a gas source (with a typical pulse length of 600 μs and a frequency of repetition of 10 Hz). The stagnation temperature was kept constant in all experiments: $T_0 = 295$ K. The stagnation pressure was varied from 50 Torr to 400 Torr. The diffusion pump (Edwards, 12 in.) provided a low background pressure ($P_{bkg} < 10^{-5}$ Torr) under all flow rates, thus excluding significant penetration of the background molecules into the free jet core. The REMPI laser beam was focused by a lens with a focal length of 15 cm onto the center streamline of the jet at some distance z_i from the exit of the nozzle. The laser radiation in the range of interest, $\lambda = 250-270$ nm ($\Delta\lambda \approx 0.01$ nm), was produced from the frequency-doubled (BBO) output of a Nd:YAG pumped dye laser (Coumarin model 503). Ions continue in the flow, interacting with neutrals in the jet core until at some distance z_f, they were extracted into the TOF mass spectrometer, using a rapidly applied transverse electric field. Typical experimental values were $z_i = 10$ mm and $z_f = 29$ mm.

State-selective ions of HBr^+ ($^2\Pi_i$, v^+) and DBr^+ ($^2\Pi_i$, v^+) were prepared by (2+1) REMPI through the $f\,^3\Delta_2$ ($v = 0$), $f\,^3\Delta_2$ ($v = 1$), $F\,^1\Delta_2$ ($v = 0$), and $F\,^1\Delta_2$ ($v = 1$) Rydberg intermediates. According to the REMPI−LIF and REMPI−PES studies of Xie and Zare,[9] REMPI through these states produces the HBr^+/DBr^+ ($^2\Pi_i$, v^+) ions almost exclusively (>98%) in one spin−orbit and vibrational state, namely ($i = {}^3/_2$, $v^+ = 0$), ($i = {}^3/_2$, $v^+ = 1$), ($i = {}^1/_2$, $v^+ = 0$), and ($i = {}^1/_2$, $v^+ = 1$), respectively. Rotational transitions for the resonance multiphoton ionization of the HBr (DBr) molecules were chosen as a compromise between intensity of a line and its isolation from lines of other isotopic analogues. In most cases, we used $R(1)$ lines and in some experiments $S(1)$. REMPI spectra of the HBr and DBr molecules through the same $f\,^3\Delta_2$ ($v = 0$) or $F\,^1\Delta_2$ ($v = 0$) intermediate states lie in the same spectral regions and we always observed some fraction of ions of the other hydrogen isotope. Moreover, low-level isotopic contamination was observed even under ionization through the $f\,^3\Delta_2$ ($v = 1$) and $F\,^1\Delta_2$ ($v = 1$) states, the spectra of which are well-separated for HBr and DBr. This is probably caused by near-resonance ionization through some other intermediate states. Despite the low percentage (<5%) of those secondary ions, they cannot be excluded from kinetic consideration until their reactivity is studied. In addition, some fraction of Br^+ ions have been observed in all ionization schemes. Their source is most probably a photodissociation of the HBr^+ and DBr^+ ions that requires only one additional photon.[11] This is confirmed by a nonlinear dependence of the Br^+ fraction on the laser power. On the other hand, the H^+ ions, which could be created in a two-photon dissociation process,[11] have never been detected in our experiments. According to this, we included in our consideration reactions with Br^+ ions and excluded those with H^+ cations.

III. Kinetics of Ion−Molecule Reactions in the HBr + DBr Free Jet

The general form of an ion−molecule reaction can be expressed as

$$I_i^+ + M_l \rightarrow I_j^+ + M_m\{k_{ij}^l\} \tag{4}$$

where I_i^+ and M_j are the ionic and neutral species, and k_{ij}^l is the rate coefficient of transformation of the ion I_i^+ to the ion I_j^+ in collision with the molecule M_l. Inputting an absolute number density of specific ions n_i^+ and neutrals n_i, an absolute number density of all ions $n^+ = \sum_i n_i^+$ and neutrals $n = \sum_i n_i$, a relative density of ions $N_i^+ = n_i^+/n$ and neutrals $N_i = n_i/n$; $\sum_i N_i^+ = \sum_i N_i = 1$, we can transform the initial set of kinetic equations for absolute densities of different species in a free jet

$$\frac{dn_i^+}{dt} = \sum_{j,l}(k_{ji}^l n_j^+ n_l - k_{ij}^l n_i^+ n_l) - n_i^+ f(t) \tag{5}$$

(where the last term describes temporal expansion in the free jet) to the set for relative values

$$\frac{dN_i^+}{dt} = n\sum_{j,l}(k_{ji}^l N_j^+ N_l - k_{ij}^l N_i^+ N_l) \tag{6}$$

Under REMPI ionization of HBr^+ (or DBr^+) ions in the (HBr + DBr) mixture, a small but finite quantity of minor ionic species (Br^+ and DBr^+, or Br^+ and HBr^+) can be observed. According to this fact, we include in our further analysis all possible reactions with all ionic species. The possible reactions are listed in Table 1, along with the 0 K reaction enthalpies. The heats of formation at $T = 0$ K for H, HBr, HBr^+, H_2Br^+,

D, DBr, Br, and Br^+ ions/species were 51.6 ± 0.1, −7 ± 0.2, 262 ± 0.5, 218 ± 0.5, 52.5 ± 0.1, −8 ± 0.2, 28.2 ± 0.1, and 300.6 ± 0.1 kcal/mol, respectively (values taken from Lias et al.[12]). The heat of formation for the DBr^+ cation was estimated as 261.9 ± 0.5 kcal/mol by comparison of the lowest internal levels of the HBr^+ and DBr^+ ions and the heats of formation for pairs (D, Br^+) and (H, Br^+). The heat of formation for the D_2Br^+ cation was estimated based on the assumption that a substitution of isotopes leads to the same effect for the (H_2Br^+, D_2Br^+) and (H_2O^+, D_2O^+) pairs:

$$\Delta_f H\{D_2Br^+\} \approx \Delta_f H\{H_2Br^+\} + \Delta_f H\{D_2O^+\} - \Delta_f H\{H_2O^+\} = 217 \pm 1 \text{ kcal/mol} \quad (7)$$

Presently available values for some rate coefficients are shown in the notes to Table 1.

The kinetics of ionic species along a free jet axis (z) is described by the following set of equations:

$$\frac{dN_1^+}{dz} = \left(\frac{n}{u}\right)(-k_1N_1^+N_1 - k_2N_1^+N_2 - k_3N_1^+N_2 + k_6N_2^+N_1 + k_7N_3^+N_1) \quad (8a)$$

$$\frac{dN_2^+}{dz} = \left(\frac{n}{u}\right)(-k_4N_2^+N_2 - k_5N_2^+N_1 - k_6N_2^+N_1 + k_3N_1^+N_2 + k_8N_3^+N_2) \quad (8b)$$

$$\frac{dN_3^+}{dz} = \left(\frac{n}{u}\right)(-k_7N_3^+N_1 - k_8N_3^+N_2) \quad (8c)$$

$$\frac{dN_4^+}{dz} = \left(\frac{n}{u}\right)k_1N_1^+N_1 \quad (8d)$$

$$\frac{dN_5^+}{dz} = \left(\frac{n}{u}\right)k_4N_2^+N_2 \quad (8e)$$

$$\frac{dN_6^+}{dz} = \left(\frac{n}{u}\right)(k_2N_1^+N_2 + k_5N_2^+N_1) \quad (8f)$$

where the fractions of the HBr and DBr molecules, $N_1 = [HBr]/n$ and $N_2 = [DBr]/n$, as well as the unique flow velocity (u) are considered to be constants over the entire reaction region from the point of ionization, z_i, to the point of detection, z_f. The gas density and the relative densities of the ions $N_1^+ = [HBr^+]/n^+$, $N_2^+ = [DBr^+]/n^+$, $N_3^+ = [Br^+]/n^+$, $N_4^+ = [H_2Br^+]/n^+$, $N_5^+ = [D_2Br^+]/n^+$, and $N_6^+ = [HDBr^+]/n^+$ are functions of the distance from the nozzle (z).

The rate coefficients k_1,..., k_8 were studied based on the kinetic equations (eqs 8) and experimental data on the relative fraction of ions (N_1^+, ..., N_6^+) produced in the reaction region between z_i and z_f. Seven signals, corresponding to the masses 79, 80, ..., 85 amu, were measured as functions of the total stagnation pressure, P_0, at every particular fraction of bromide molecules, $(N_1 + N_2) = ([HBr] + [DBr])/n$. Two sets of experiments were performed. In the first set, referenced below as (SET I), the (2+1) REMPI of HBr^+ was used in the He + HBr + DBr mixtures with the ratio of $[HBr]/[DBr] \approx 3.7 \pm 0.2$ and total fraction of bromides from 0.32% ± 0.02% to 2.0% ± 0.1%. In the second one, referenced hereafter as (SET II), the (2+1) REMPI of DBr^+ was explored under $[HBr]/[DBr] \approx 0.37 \pm 0.02$ and a total fraction of bromides in the same limits. All these measurements were repeated for each path of ionization, using the Rydberg intermediate states $f\ ^3\Delta_2[^2\Pi_{3/2}, v = 0]$; $f\ ^3\Delta_2[^2\Pi_{3/2}, v = 1]$; $F\ ^1\Delta_2[^2\Pi_{1/2}, v = 0]$; $F\ ^1\Delta_2[^2\Pi_{1/2}, v = 1]$. Because of the small difference between ion masses (compared to their absolute values), an equal collection/detection efficiency was assumed. Ratios between measured signals then represent ratios between fractions of corresponding ions. Thus, the signals from masses of 79, 80, ..., 85, normalized by the sum of all signals, represent the fractions of the $^{79}Br^+$, $H^{79}Br^+$, ($^{81}Br^+ + D^{79}Br^+ + H_2{}^{79}Br^+$), ($H^{81}Br^+ + HD^{79}Br^+$), ($H_2{}^{81}Br^+ + D^{81}Br^+ + D_2{}^{79}Br^+$), $HD^{81}Br^+$, $D_2{}^{81}Br^+$ ions in the extraction point of the flow. In the notation of eq 8, they are $N_3^+/2$, $N_1^+/2$, ($N_3^+ + N_2^+ + N_4^+$)/2, ($N_1^+ + N_6^+$)/2, ($N_4^+ + N_2^+ + N_5^+$)/2, $N_6^+/2$, and $N_5^+/2$, assuming equal concentration of $X^{79}Br^+$ and $X^{81}Br^+$ ions that are dependent on the initial ratios $[H^{79}Br]/[H^{81}Br]$ and $[D^{79}Br]/[D^{81}Br]$, as well as on ionization wavelength, and will be verified for our conditions below.

IV. Numerical Simulation

Almost all differential equations of the system (eqs 8), excluding eq 8c, contain interference with each other and cannot be integrated analytically in their original form. To derive relations between the rate coefficients and experimental data, we need to simplify some of eqs 8. As a first step of analysis, a numerical integration of eqs 8 was conducted. All eight reactions listed in Table 1 were simulated numerically. The flow was considered as a uniform gas mixture with a constant fraction of all original molecules (He, HBr, DBr) from the nozzle to an extraction point. Gas parameters were considered to obey the "spherical expansion" model.[13] The entire reaction region (between $z_i = 10$ mm and $z_f = 29$ mm, i.e., $z_i/D = 25$ and $z_f/D = 72$) belongs to the so-called "hypersonic" component of the flow; therefore, the flow velocity u is approximately constant and the number density n is well-described by the formula $n = n_0z_0^2/z^2$, where n_0 is the stagnation gas density and $z_0 = aD$ (D is the nozzle diameter and $a = 0.401$ and 0.298 for monatomic and diatomic gases, respectively).

Equations 8 were integrated numerically, beginning from the point of ionization, z_i, where a fraction of each ion was considered to be a parameter: $N_1^+(z_i) = a_{HBr^+}$, $N_2^+(z_i) = a_{DBr^+}$, and $N_3^+(z_i) = a_{Br^+}$ and $N_4^+(z_i) = 0$, $N_5^+(z_i) = 0$, and $N_6^+(z_i) = 0$. The fraction of the minor ionic species (Br^+, DBr^+ in SET I and Br^+, HBr^+ in SET II) was not large (usually <5%) and they were not able to affect product distributions of the primary reactions dramatically. However, their role in secondary reactions was significant. For example, under resonant ionization of the HBr^+ ions, there is a low probability that the presence of some portion of the DBr^+ and Br^+ ions is important in determining the kinetics of the HBr^+ and H_2Br^+ ions. However, even their low fraction may be dominant in the kinetics of the D_2Br^+. The original (at the point of ionization, z_i) fraction of the ions a_{HBr^+}, a_{DBr^+}, and a_{Br^+} (which is considered to be independent of the stagnation pressure, P_0, but dependent on ionization wavelength) and the rate coefficients k_1,..., k_8 (which are considered to be independent of temperature, but again, dependent on the internal state of the ions created) were taken as parameters of numerical integration and were determined by a best fit to the experimental data.

The results of this optimization are shown in Table 1 (in square brackets) and provide an approximate estimation for the rate coefficients, because the efficiency and accuracy of the multiparametric fitting decreases sharply with the number of parameters and places high demands on the accuracy and the body of experimental data. The second goal of the simulation

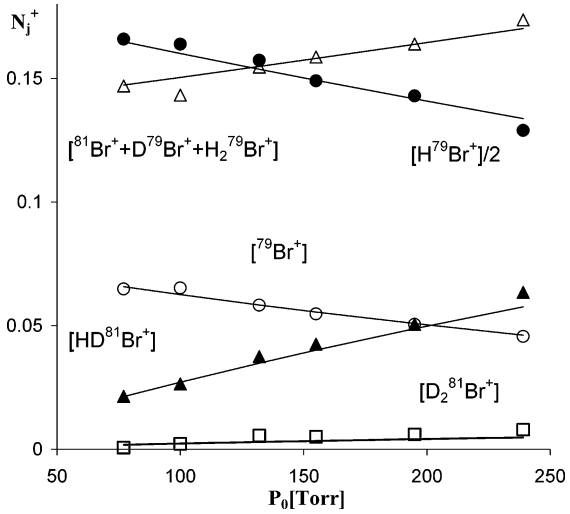

Figure 1. Comparison of measured (symbols) and simulated (lines) fractions of ions at the point of their extraction for (2+1) REMPI of HBr^+ through the $f\,^3\Delta_2(v = 0)$ intermediate state in the He + HBr-(1.6%) + DBr(0.4%) mixture. The rate coefficients used are presented in Table 1.

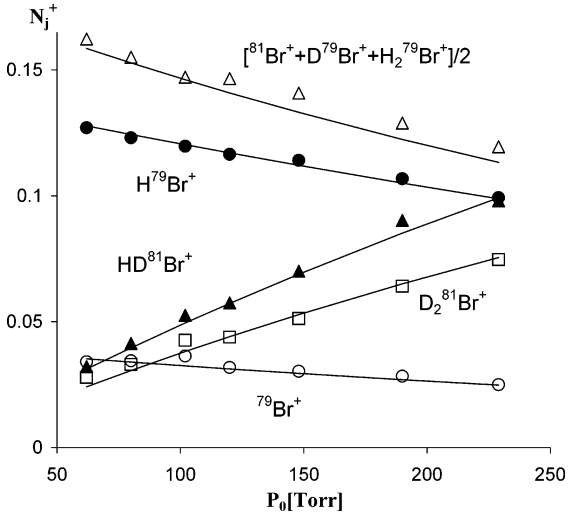

Figure 2. Comparison of measured (symbols) and simulated (lines) fractions of ions at the point of their extraction for (2+1) REMPI of DBr^+ through the $F\,^1\Delta_2(v = 0)$ intermediate state in the He + HBr-(0.6%) + DBr(1.7%) mixture.

was to investigate the importance of individual reactions in the kinetics of ions and to justify a procedure of simplification of eqs 8 for more-accurate derivation of the rate coefficients. An example of the comparison between the simulation results and the experimental data is shown in Figures 1 and 2 for the data of SET I and SET II, respectively.

V. Analytical Solution

Fractions of Ions in the Ionization Region. First, we define the initial fractions of the HBr^+, DBr^+, and Br^+ ions (a_{HBr^+}, a_{DBr^+}, and a_{Br^+}, respectively) in the point of ionization z_i separately for the ^{79}Br and ^{81}Br isotopic species. They were derived from extrapolation of the corresponding mass-spectrometric signals to $P_0 = 0$. Extrapolation of the signals S_{79}, S_{80}, S_{81}, S_{82}, and S_{83} gives the values of $a^{(79)}_{Br^+}$, $a^{(79)}_{HBr^+}$, $a^{(81)}_{Br^+} + a^{(79)}_{DBr^+}$, $a^{(81)}_{HBr^+}$, $a^{(81)}_{DBr^+}$, respectively, where the superscripts indicate the isotopic mass of Br in an ion. These variables can be observed as a limiting case ($n \to 0$) of the data shown in Figures 1−6. The initial ionic fractions found from these data are listed in Table 2 for every ionization path. Because the values of $a^{(81)}_{Br^+}$ and $a^{(79)}_{DBr^+}$ cannot be found independently, we have assumed that a minor species has the same isotopic fractions: in the case of (2+1) REMPI of HBr^+ (SET I), the $a^{(79)}_{DBr^+}$ value was assumed to be equal to the $a^{(81)}_{DBr^+}$ value and the $a^{(81)}_{Br^+}$ value was derived from extrapolation of the S_{81} signal; whereas in the case of (2+1) REMPI of DBr^+ (SET II) the $a^{(81)}_{Br^+}$ was assumed to be equal to the $a^{(79)}_{Br^+}$ and the $a^{(79)}_{DBr^+}$ was found from $a^{(81)}_{Br^+} + a^{(79)}_{DBr^+}$. As shown in Table 2, all isotope-substituted ions have similar fractions in all cases with a small predominance of light species that, however, is inside the error limits.

Now we can express the experimentally measured ion signals through the rate coefficients and flow parameters by integration of eqs 8.

Kinetics of the Br^+ Ions. Equation 8c can be simply integrated in the region between z_i and z_f, giving

$$N_3^+(z_f) = a_{Br^+}\exp\left[-n_0 z_0^2\left(\frac{1}{z_i} - \frac{1}{z_f}\right)\left(\frac{k_7 N_1 + k_8 N_2}{u}\right)\right] \quad (9a)$$

or

$$\ln(N_3^+) = \ln(a_{Br^+}) - k_{78}\zeta \quad (9b)$$

where $k_{78} = k_7\eta + k_8\delta$ and ζ is the reaction-time-integrated number density ($\zeta = (N_1 + N_2)\{n_0 z_0^2[(1/z_i) - (1/z_f)]/u\}$), which is related to the number of collisions experienced between the ionization point and the detection point in the jet; $\eta = N_1/(N_1 + N_2)$ and $\delta = N_2/(N_1 + N_2)$. Using the variable ζ gives an opportunity for joint analysis of all experimental data obtained under various total fractions of bromides, $(N_1 + N_2)$, if the ratio N_1/N_2 is kept constant.

Kinetics of the HBr^+ and DBr^+ Ions. Integration of other equations from the set of equations (eqs 8) requires some simplification of them. Note that the set of reactions listed in Table 1, as well as the set of equations (eqs 8) are symmetric, relative to isotope-substituted species, and can be transformed by substitution H ⇔ D in every ionic and neutral particle with consequent substitution of the rates: (k_1, k_2, k_3, k_7) ⇔ (k_4, k_5, k_6, k_8). Thus, we consider in detail only the kinetic equations for the case of (2+1) REMPI of HBr^+ in the [HBr]/[DBr] = 3.7 mixtures (SET I). Corresponding expressions for the ion kinetics under (2+1) REMPI of DBr^+ in the [HBr]/[DBr] = 0.37 mixtures (SET II) can be obtained by consequent substitutions.

As a first approximation, eq 8a was integrated, neglecting the fourth and fifth terms, which describes an additional portion of the HBr^+ ions produced in charge-transfer reactions R6 and R7 (refer to Table 1). In this case, the kinetics of the HBr^+ ions is presented:

$$N_1^+(\zeta) = a_{HBr^+}\exp(-k_{123}\zeta) \quad (10)$$

where the effective rate coefficient $k_{123} = k_1\eta + k_2\delta + k_3\delta$. This seems to be a correct approximation for data analysis of the SET I experiments, where $a_{HBr^+} \gg (a_{DBr^+}, a_{Br^+})$ and δ is significantly higher than η. A corresponding expression for the kinetics of the DBr^+ ions in the SET II experiments is

$$N_2^+(\zeta) = a_{DBr^+}\exp(-k_{456}\zeta) \quad (11)$$

with the effective rate coefficient $k_{456} = k_4\delta + k_5\eta + k_6\eta$.

Considering the kinetics of the minor isotopic ions (DBr^+ in SET I or HBr^+ in the SET II experiments), we must take into

TABLE 2: Initial Fraction of the HBr^+, DBr^+, and Br^+ Ions at the Point of Ionization, z_i, under Different Ionization Schemes

	Fraction of Ions			
	$f\,^3\Delta[^3/_2, v=0]$	$f\,^3\Delta[^3/_2, v=1]$	$F\,^1\Delta[^1/_2, v=0]$	$F\,^1\Delta[^1/_2, v=1]$
	Ionization of HBr^+			
$a^{(79)}_{HBr^+}$	0.383 ± 0.020	0.374 ± 0.022	0.402 ± 0.030	0.289 ± 0.019
$a^{(81)}_{HBr^+}$	0.383 ± 0.021	0.348 ± 0.023	0.396 ± 0.032	0.246 ± 0.018
$a^{(79)}_{DBr^+}$	0.032 ± 0.007	0.018 ± 0.005	0.036 ± 0.008	0.053 ± 0.011
$a^{(81)}_{DBr^+}$ [a]	0.032	0.018	0.036	0.053
$a^{(79)}_{Br^+}$	0.084 ± 0.008	0.134 ± 0.012	0.085 ± 0.012	0.182 ± 0.016
$a^{(81)}_{Br^+}$	0.074 ± 0.007	0.115 ± 0.011	0.060 ± 0.010	0.178 ± 0.016
$Sum^{(79)}$	0.499 ± 0.024	0.526 ± 0.026	0.523 ± 0.032	0.524 ± 0.025
$Sum^{(81)}$	0.489 ± 0.025	0.481 ± 0.027	0.492 ± 0.034	0.477 ± 0.026
	Ionization of DBr^+			
$a^{(79)}_{HBr^+}$	0.069 ± 0.010	0.104 ± 0.012	0.122 ± 0.014	0.108 ± 0.011
$a^{(81)}_{HBr^+}$	0.065 ± 0.010	0.101 ± 0.013	0.119 ± 0.013	0.107 ± 0.011
$a^{(79)}_{DBr^+}$	0.399 ± 0.026	0.330 ± 0.021	0.325 ± 0.022	0.320 ± 0.020
$a^{(81)}_{DBr^+}$	0.407 ± 0.025	0.305 ± 0.021	0.336 ± 0.023	0.335 ± 0.020
$a^{(79)}_{Br^+}$	0.017 ± 0.006	0.080 ± 0.014	0.042 ± 0.011	0.058 ± 0.011
$a^{(81)}_{Br^+}$ [b]	0.017	0.080	0.042	0.058
$Sum^{(79)}$	0.485 ± 0.030	0.514 ± 0.028	0.489 ± 0.027	0.486 ± 0.025
$Sum^{(81)}$	0.489 ± 0.029	0.486 ± 0.026	0.497 ± 0.026	0.500 ± 0.025

[a] $a^{(81)}_{DBr^+}$ was assumed to be equal to $a^{(79)}_{DBr^+}$. [b] $a^{(81)}_{Br^+}$ was assumed to be equal to $a^{(79)}_{Br^+}$.

account all terms of eqs 8a and 8b, because the importance of the fourth and/or fifth terms is quite possible here. Integration of eq 8a using eq 9a for a fraction of the Br^+ ions, $N_3^+(z)$, and eq 11 for a fraction of the DBr^+ ions, $N_2^+(z)$, gives

$$N_1^+(\zeta) = \exp(-k_{123}\zeta)\left\{a_{HBr^+} + \frac{a_{DBr^+}k_6\eta}{k_{456}-k_{123}}[1-\exp(k_{123}-k_{456})\zeta] + \frac{a_{Br^+}k_7\eta}{k_{78}-k_{123}}[1-\exp(k_{456}-k_{78})\zeta]\right\} \quad (12)$$

The corresponding expression for the DBr^+ ions in the experiments of SET I is

$$N_2^+(\zeta) = \exp(-k_{456}\zeta)\left\{a_{DBr^+} + \frac{a_{DBr^+}k_3\delta}{(k_{123}-k_{456})}[1-\exp(k_{456}-k_{123})\zeta] + \frac{a_{Br^+}k_8\delta}{k_{78}-k_{456}}[1-\exp(k_{456}-k_{78})\zeta]\right\} \quad (13)$$

Certainly, eqs 12 and 13 describe the kinetics of the HBr^+ and DBr^+ ions in both experimental sets rather well; however, they are absolutely inappropriate for analysis of experimental data, especially for the kinetics of the H_2Br^+, D_2Br^+, and $HDBr^+$ ions, because integration of eqs 8d−f leads to multiterm expressions that include all eight rate coefficients. Instead of them, considering results of SET I, we will use eq 10 for the HBr^+ ions, that answer to the first term in eq 12, and a linearized approximation of eq 13 for the DBr^+ ions

$$N_2^+(\zeta) \approx a_{DBr^+} + a_{HBr^+}k_3\delta\zeta + a_{Br^+}k_8\delta\zeta \quad (14)$$

that is based on the following experimental conditions: $a_{HBr^+} \gg (a_{DBr^+}, a_{Br^+})$, $\delta/\eta = 3.7$, and $k_i\zeta \ll 1$ for all rate coefficients k_i. The kinetics of the DBr^+ and HBr^+ ions in the SET II experiments is considered, based on eqs 11 and 15, respectively:

$$N_1^+(\zeta) \approx a_{HBr^+} + a_{DBr^+}k_6\eta\zeta + a_{Br^+}k_7\eta\zeta \quad (15)$$

Kinetics of the H_2Br^+, $HDBr^+$, and D_2Br^+ Ions. Now we consider the kinetics of other minor ionic species. In both experimental sets, they are H_2Br^+, $HDBr^+$, and D_2Br^+. Evolution of the H_2Br^+ ions, N_4^+, is described by eq 8d, using $N_1^+(\zeta)$ from eq 10 for SET I and from eq 15 for SET II. Integration of eq 8d gives

$$N_4^+(\zeta) = \frac{a_{HBr^+}\eta k_1[1-\exp(-k_{123}\zeta)]}{k_{123}} \approx a_{HBr^+}\eta k_1\zeta \quad (16)$$

for SET I and

$$N_4^+(\zeta) = \eta k_1\zeta\left(\frac{a_{HBr^+} + a_{DBr^+}\eta k_3\zeta}{2} + \frac{a_{Br^+}\eta k_7\zeta}{2}\right) \quad (17)$$

for SET II. Analogously, the kinetics of the D_2Br^+ ions is described by

$$N_5^+(\zeta) = \frac{a_{DBr^+}\delta k_4[1-\exp(-k_{456}\zeta)]}{k_{456}} \approx a_{DBr^+}\delta k_4\zeta \quad (18)$$

and

$$N_5^+(\zeta) = \delta k_4\zeta\left(\frac{a_{DBr^+} + a_{HBr^+}\delta k_6\zeta}{2} + \frac{a_{Br^+}\delta k_8\zeta}{2}\right) \quad (19)$$

respectively. At last, the kinetics of the $HDBr^+$ ions (N_6^+) is described by eq 8f, which, after integration by the same manner and simplification to linear terms only, leads to the expression

$$N_6^+(\zeta) = (a_{HBr^+}\delta k_2 + a_{DBr^+}\eta k_5)\zeta = k_{25}\zeta \quad (20)$$

Thus, a fraction of the ionic species Br^+, HBr^+, DBr^+, H_2Br^+, D_2Br^+, and $HDBr^+$, at the point of extraction z_f, is described by eq 9, eq 10 or 15, eq 11 or 14, eqs 16 and 17, eqs 18 and 19, and eq 20, respectively.

VI. Rate Coefficients

Charge-Transfer Reaction: $Br^+ + HBr\ (DBr) \rightarrow Br + HBr^+\ (DBr^+)$ and Rate Coefficients k_7 and k_8. Br^+ ions disappear in reactions 7 and 8 (see Table 1), according to eq 9. The experimental data of SET I and SET II are shown in Figure 3. Here, and below, we present only results for REMPI of the HBr and DBr molecules through the $F\,^1\Delta_2[^2\Pi_{1/2}, v=1]$ states,

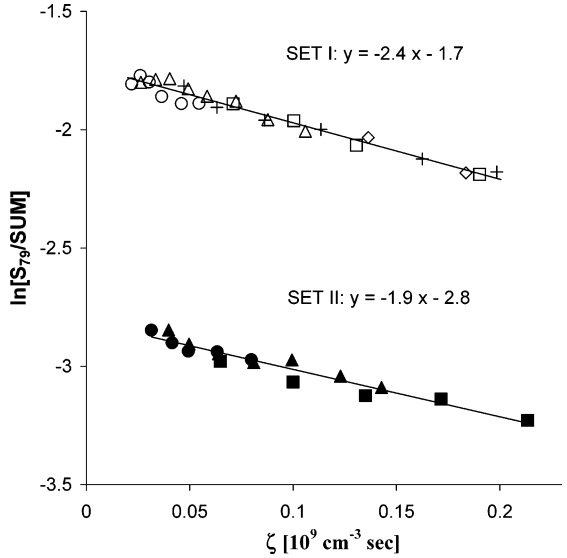

Figure 3. Kinetics of the Br^+ ions, observed by the signal of mass 79 (S_{79}), as a function of the number of collisions with the bromide molecules. Open symbols represent (2+1) REMPI of HBr^+ through the $F\ ^1\Delta_2$ ($v = 1$) Rydberg state in the He + HBr + DBr mixture with the constant ratio [HBr]/[DBr] = 3.7 and various total fractions of bromides ((◇) 3.2%, (□) 2.0%, (△) 1.0%, (+) 0.6%, and (○) 0.4%). Closed symbols represent (2+1) REMPI of DBr^+ through the $F\ ^1\Delta_2$ ($v = 1$) state in the mixture with the ratio [HBr]/[DBr] = 0.37 and various total fractions of bromides ((■) 2.4%, (▲) 1.1%, and (●) 0.5%). Lines are the best linear approximations of the data.

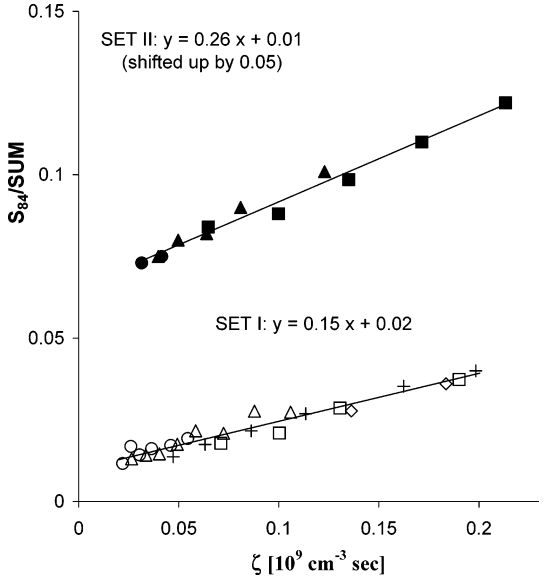

Figure 4. Kinetics of the $HDBr^+$ ions (S_{84}) in experiments of SET I (open symbols) and SET II (closed symbols). Experimental conditions and symbols are the same as those given in Figure 3.

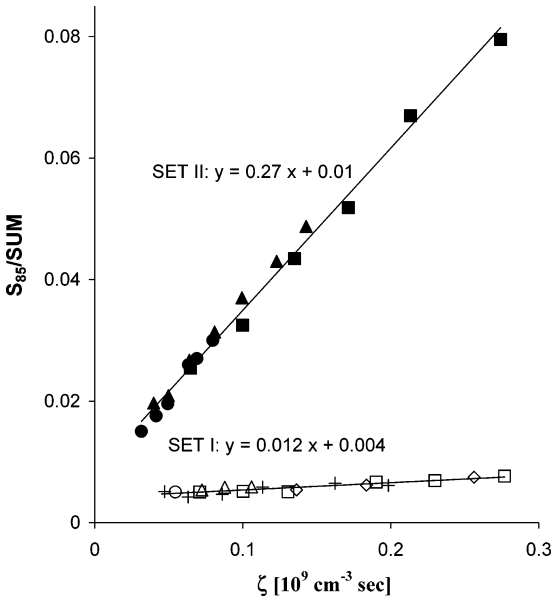

Figure 5. Kinetics of the D_2Br^+ ions (S_{85}) in experiments of SET I (open symbols) and SET II (closed symbols). Experimental conditions and symbols are the same as those given in Figure 3.

because other data are qualitatively the same. The ratio [HBr]/[DBr] = 3.7 (SET I) and 0.37 (SET II) was kept constant inside one set and the total fraction of bromides in the He + HBr + DBr mixture was varied from 0.4% to 3.2%. The S_{79} signal, corresponding only to the $^{79}Br^+$ ion, was used here, because, as shown previously, the fractions of the $^{79}Br^+$ and $^{81}Br^+$ ions are almost the same and the $^{81}Br^+$ signals are interfered by the $H_2{}^{79}Br^+$ and $D^{79}Br^+$ signals. The effective rate coefficient ($k_{78} = k_7\eta + k_8\delta$), as well as the initial fraction of Br^+ ions (a_{Br^+}), were derived from the slope and intersection with the axis $\zeta = 0$ in Figure 3, according to eq 9b. The actual rate coefficients for reactions 7 and 8 (see Table 1) then were obtained by comparison of k_{78}(SET I) and k_{78}(SET II). The results seem to be independent of the ionization path: k_7 (in units of 10^{-9} cm^3/s) = 2.7 ± 0.4, 2.7 ± 0.4, 2.8 ± 0.4, and 2.6 ± 0.4 and k_8 (also in units of 10^{-9} cm^3/s) = 1.6 ± 0.3, 1.6 ± 0.3, 1.7 ± 0.3, and 1.6 ± 0.3 for ionization through the $f\ ^3\Delta_2$ ($v = 0$), $f\ ^3\Delta_2$ ($v = 1$), $F\ ^1\Delta_2$ ($v = 0$), and $F\ ^1\Delta_2$ ($v = 1$) states.

Reaction of $HDBr^+$ Production: $HBr^+(DBr^+)$ + DBr-(HBr) → $HDBr^+$ + Br and Rate Coefficients k_2 and k_5. The rate coefficients k_2 and k_5 were determined by comparison of k_{25} measured in two experimental sets, and k_{25} was derived, according to eq 20, from $S_{84}(\zeta)$, which represents the fraction of $HD^{81}Br^+$ isotope. In the case of DBr^+ REMPI (SET II), when the fraction of HBr^+ ions is small, additional information about the kinetics of N_6^+ was received from a combination of other signals:

$$S_{82} - S_{80} = \frac{[H^{81}Br^+] + [HD^{79}Br^+] - [H^{79}Br^+]}{\Sigma(I^+)} \approx \frac{N_6{}^+}{2} \quad (21)$$

where $\Sigma(I^+)$ is the sum of all ions. The dependencies of the S_{84} ion signals on the integrated number density of hydrogen bromides, ζ, are shown in Figure 4 for SET I and SET II. In the ($\Pi_{3/2}$, $v = 0$), ($\Pi_{3/2}$, $v = 1$), ($\Pi_{1/2}$, $v = 0$), and ($\Pi_{1/2}$, $v = 1$) states, the k_2 and k_5 values (× 10^{-9} cm^3/s, ±20%) were 1.7, 1.7, 1.6, and 1.6 for the HBr^+ ions, and 1.6, 1.7, 1.5, and 1.5 for the DBr^+ ions, respectively. Actually, the determined rate coefficients k_2 represent an average rate of the $H^{79}Br^+/D^{81}Br$ H^+-transfer and the $H^{81}Br^+/D^{79}Br$ D-transfer processes, which are inseparable in our experiments, and the rate coefficient k_5 represents the $D^{79}Br^+/H^{81}Br$ D^+-transfer and the $D^{81}Br^+/H^{79}Br$ H-transfer reactions.

Reaction of D-atom and/or D^+-ion Transfer: DBr^+ + DBr → D_2Br^+ + Br and Rate Coefficient k_4. One more rate coefficient can be derived directly from the experimental data. It is k_4 that representsreaction R4 from Table 1. Figure 5 presents data on evolution of the S_{85} signal that corresponds to the $D_2{}^{81}Br^+$ ions. These data are linear in all investigated ranges of ζ for both experimental sets, which justifies use the linear approximation in eq 18 or the first term of eq 19 for interpretation of the data of both experimental sets. Taking into

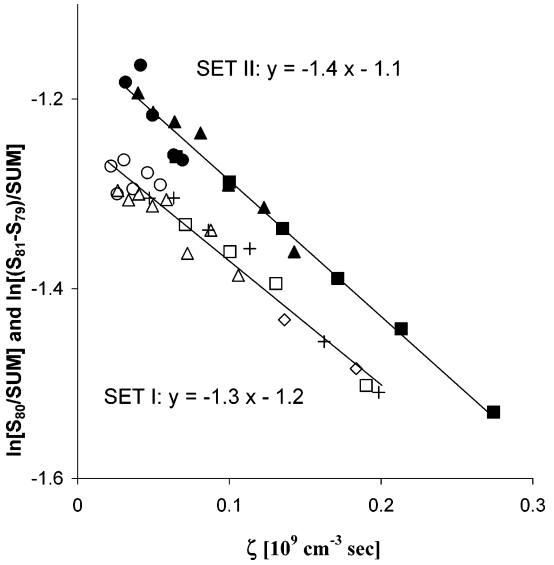

Figure 6. Kinetics of the HBr^+ ions in SET I (open symbols) and of the ($DBr^+ + H_2Br^+$) ions in SET II (closed symbols). Experimental conditions and symbols are the same as those given in Figure 3.

account values of a_{DBr^+}(SET I), a_{DBr^+}(SET II), δ(SET I), and δ(SET II), we receive $k_4(\times 10^9$ cm^3/s) = 1.5, 1.3, 1.4, and 1.1 ($\pm$24%) from SET I and 1.4, 1.1, 1.4, and 1.1 ($\pm$17%) from SET II for the DBr^+ ($\Pi_{3/2}$, $v = 0$), ($\Pi_{3/2}$, $v = 1$), ($\Pi_{1/2}$, $v = 0$), and ($\Pi_{1/2}$, $v = 1$) states, respectively.

Effective Rate Coefficients for Kinetics of HBr^+ and DBr^+ Ions and Rate Coefficients k_1, k_3, and k_6. The rate coefficients k_1, k_3, and k_6 cannot be found from our experiments directly. Their estimation is based on the kinetics of HBr^+ and DBr^+ ions and the rate coefficients found previously. Loss of the HBr^+ ions in experiments of SET I is shown in Figure 6. The data were analyzed using eq 10, with an effective rate coefficient $k_{123}^{(I)} = (k_1\eta^{(I)} + k_2\delta^{(I)} + k_3\delta^{(I)})$, which was found as $k_{123}^{(I)}(\times 10^{-9}$ cm^3/s) = 1.5, 1.3, 1.5, and 1.3 ($\pm$15%) for the $H^{79}Br$ ($\Pi_{3/2}$, $v = 0$), ($\Pi_{3/2}$, $v = 1$), ($\Pi_{1/2}$, $v = 0$), and ($\Pi_{1/2}$, $v = 1$) ions. The intersection of the data with the ordinate axis also gives the values of $a_{HBr^+}^{(I)}$ presented in Table 2. The rate coefficient $k_{456}^{(II)} = k_4\delta^{(II)} + k_5\eta^{(II)} + k_6\eta^{(II)}$ that describes loss of DBr^+ ions has been found from the corresponding data of SET II. Because both signals of the $D^{79}Br^+$ and $D^{81}Br^+$ ions were intervened with other ions of the same masses, we used a combination

$$S_{81}^{(II)} - S_{79}^{(II)} = [^{81}Br^+] + [D^{79}Br^+] + [H_2{}^{79}Br^+] - [^{79}Br^+] \approx \frac{N_2^+}{2} + \frac{N_4^+}{2} \approx \frac{N_2^+}{2} \quad (22)$$

and neglected the contribution of the $H_2{}^{79}Br^+$ ions, which was <5% as it was estimated by comparison of D_2Br^+ and HBr^+ signals (S_{85} and S_{80}) in the SET I experiments. The second set of data in Figure 6 presents the data for definition of the rate coefficient $k_{456}^{(II)}$ and value of $a_{DBr+}^{(II)}$ from eq 11. For the ($\Pi_{3/2}$, $v = 0$), ($\Pi_{3/2}$, $v = 1$), ($\Pi_{1/2}$, $v = 0$), and ($\Pi_{1/2}$, $v = 1$) states of the $D^{79}Br^+$ ions, the effective rate coefficients $k_{456}^{(II)}$ ($\times 10^{-9}$ cm^3/s, $\pm$15%) were 1.6, 1.5, 1.4, and 1.4, respectively.

The rate coefficient k_6 can be derived from $k_{456}^{(II)}$, taking into account values of k_5 and k_4 previously given in Section VI: $k_6 = (6 \pm 3) \times 10^{-10}$ cm^3/s for all states of the DBr^+ ions. If we assume a similar value for the reverse reaction (that is confirmed by the results of Green et al.[3] and Xie and Zare[9]), the rate coefficient k_1 of the reaction of the H-atom and/or H^+-ion transfer (R1) can be found from k_{123}: $k_1(\times 10^{-9}$ cm^3/s) = 1.3, 1.0, 1.3, 1.1 for the ($\Pi_{3/2}$, $v = 0$), ($\Pi_{3/2}$, $v = 1$), ($\Pi_{1/2}$, $v = 0$) and ($\Pi_{1/2}$, $v = 1$) ionic states. Accuracy of this derivation was estimated as 25%, because of low and very low weights of the terms that contain the rate coefficients k_2 and k_3, respectively.

VII. Analysis and Discussion

The rate coefficients of reactions R1−R8, listed in Table 1, have been determined to be the best fits of eqs 9b, 10, 11, 14−18, and 20 to the final fraction of ions measured in the experiment. As expected, both procedures (simulation and direct kinetics) have led to similar results. Wider error limits for the rates found by the simulation procedure are explained by some uncertainty in the statistical weights that have been chosen for ionic species in the fitting procedure. Accuracy of the rates found from Figures 3−6 is defined by applicability of the assumed kinetic model to our experimental conditions, as well as by accuracy of the measurements of the final ion fractions and the value of $\zeta = (N_1 + N_2)[n_0 z_0^2(1/z_i - 1/z_f)/u]$. Processes such as clustering or quenching of the excited states were excluded from our consideration, based on the fact that the kinetics of the ions was dependent only on the parameter ζ under a variety of particular experimental conditions, such as the position of ionization and detection points or the number density of individual gas species. The parametrization of the data indicates that (i) they are the result of binary collisions of bromides, which are not subject to quench by or charge transfer to the He atoms; and (ii) the gas density in the flow obeys the spherical expansion model without an observable effect of flow heating by condensation. In addition, the appearance of cluster ions was easily determined and controlled by mass spectrometry. In regard to quenching of the excited spin−orbit and vibrational states of the ions, it is difficult to imagine a channel that involves anything other than vibrational excitation of neutral hydrogen bromides. The rates of these energy transfer channels are unknown but are expected to be slow; that hypothesis is supported by the lack of evidence for any of measured rates, depending upon the mole fraction of hydrogen bromide. However, we cannot exclude energy transfer to HBr/DBr and, in this case, the measured rate coefficients for the excited ions must be considered only as their upper limits. Most of the expressions are derived from exact equations in the "low-density" approximation, which is justified for our experimental conditions if values of the rates are not too high ($k \approx 10^{-9}$ cm^3/s or less). A contribution of every neglected term to the final fraction of ions was verified by a numerical simulation procedure. Thus, it has been established that the simplified equations work rather well. Uncertainty in the rate coefficients caused by scattering of the ion fraction data can be estimated as 3%−15% (see Figures 3−6).

Actual accuracy of the ζ value is defined by applicability of the gas-dynamic model assumed rather than by the accuracy of values measured. The latter errors were estimated as follows: 5%−7% for the bromide fractions N_1 and N_2; < 3% for the stagnation density n_0; and 5% for the distances z_i and z_f. The "spherical expansion" model works very well to describe gas density in a free jet. Accuracy of this description was checked in many experimental studies,[13,14] and errors can be estimated as <3%. The situation with gas temperature and flow velocity is more complicated; however, they are also very important in defining the reaction time (as TOF between the ionization and extraction points) and the temperature, to which the measured rate coefficients should be attached. They are still very predictable in the initial equilibrium portion of the flow. Far from the

nozzle, however, the equilibrium between different energy modes is disturbed and the concept of temperature is lost. Moreover, aerodynamic separation of gases in seeded free jets[15,16] leads to velocity and temperature slip between light and heavy fractions. In speaking about a translational temperature, we can introduce parallel and perpendicular temperatures ($T_{\|}$ and $T_{\perp}$, respectively) as a measure of velocity dispersion along and across a free jet axis. These temperatures, as well as the flow velocity, can be estimated in the He + HBr(2%) free jet, using the results of Tanaka et al.[17] for the He + Kr(2%) mixture (because the masses of HBr and Kr are very similar). For the same stagnation temperature ($T_0 = 295$ K) and variation of P_0D (20−80 Torr mm, which is the range of our experiments), they observed $T_{\|}^{He}$ (from 14 to 3 K), $T_{\|}^{Kr}$ (from 38 to 9 K), and $\Delta u/u_{is}$ (from 0.12 to 0.09), where u_{is} is the isentropic terminal velocity and Δu is the difference between velocity of the light and that of the heavy species (velocity slip). The isentropic terminal flow velocity in the helium free jet seeded by HBr with the molar fraction α can be determined from a simple energy balance. Neglecting the small portion of energy that remains in the rotational degrees of freedom, we can write

$$\frac{k_B T_0 \gamma}{\gamma - 1} = \frac{(1-\alpha) m_{He} u_{is}^2}{2} + \frac{\alpha m_{HBr} u_{is}^2}{2} \qquad (23)$$

where k_B is the Boltzmann constant, γ is the heat-capacity ratio for the mixture ($\gamma = (2\alpha + 5)/(2\alpha + 3)$), T_0 is the stagnation temperature, and m_{HBr} and m_{He} are the molecular masses. For the fraction of HBr, $\alpha = 0.01$ and 0.02, the isentropic flow velocities are $u_{is} = 1.60 \times 10^5$ and 1.49×10^5 cm/s, respectively. The velocity of the HBr^+/DBr^+ ions between the point of ionization z_i and the point of extraction z_f was measured by the delay between pulses of the ionization laser and the sweeping field. Typical values of the velocity were $u_{HBr^+} = 1.2 \times 10^5$ and 1.1×10^5 cm/s for $\alpha = 0.01$ and 0.02, respectively, which demonstrates slightly higher velocity slip effects, compared to the data of Tanaka et al.[17]

Looking at the measured rate coefficients, listed in Table 1, we first notice the relatively high rate ($\sim 10^{-9}$ cm^3/s) of all the reactions studied. This is entirely consistent with the fact that all the reactions are exothermic and occur on potential surfaces that contain strong ion−dipole interactions. Considering the rate coefficients for the ion−dipole capture, Su and Bowers[4] gave the following expression:

$$k = 2\pi q \left(\frac{\alpha_p}{\mu}\right)^{1/2} \left[1 + c\mu_D \left(\frac{2}{\pi k T \alpha_p}\right)^{1/2}\right] \qquad (24)$$

where q is the charge on the ion, α_p the polarizability of the molecule, μ the reduced mass, μ_D the dipole moment of the molecule, k the Boltzmann's constant, T the absolute temperature, and c the degree of orientation of the dipole in the ion field. For the case of $c = 0$, in regard to the ion-induced dipole interaction, the relationship (providing a lower limit of the ion−dipole capture) is independent of temperature; for the (Br^+, HBr^+, DBr^+)−(HBr, DBr) pairs, the relation is equal to 7×10^{-10} cm^3/s. The simplest model that accounts for the ion−dipole interaction is probably the locked dipole (LD) approximation that has been treated by Theard and Hamill[18] and Moran and Hamill,[19] which is consequent to $c = 1$ in eq 24. In this case, the rate coefficient for our ion−molecule pairs increases from $k_{LD}(T = 300\ K) = 2 \times 10^{-9}$ cm^3/s to $k_{LD}(T = 10\ K) = 7 \times 10^{-9}$ cm^3/s. Because the ion field cannot completely freeze the rotational angular momentum of the polar molecule, the LD approximation provides only an upper limit to the ion−dipole capture rate coefficient that overestimates (sometimes, seriously) the dipole effect.[20] The average dipole orientation (ADO) model is more realistic, providing a good agreement with many experiments.[4] For the (Br^+, HBr^+, DBr^+)−(HBr, DBr) ion−molecule interaction, the rate coefficients are $k_{ADO}(T = 300\ K) = 9 \times 10^{-10}$ cm^3/s to $k_{ADO}(T = 10\ K) = 3 \times 10^{-9}$ cm^3/s (here, we used $c(300\ K) = 0.18$ and $c(10\ K) = 0.3$, according to ref 4).

A theory of ion−dipolar molecule interaction was also developed and the ion−molecule capture rates were calculated by Su and Chesnavich,[21] Su,[22,23] Clary,[24] Clary et al.,[25] Rebrion et al.,[26] and Troe.[27,28] Tests on the same ion−molecule pairs demonstrate good agreement between these approaches at temperatures of 100 K and higher, where they describe the experiment very well,[24,26,27] whereas the ADO rates are ~30% lower. At lower temperatures, the classical trajectory[23] and statistical adiabatic channel models[27] give similar results up to 5 K, whereas the rates calculated by adiabatic capture−centrifugal sudden approximation[25] demonstrate a stronger temperature dependence. However, any more-extensive comparison of our experimental rate coefficients does not seem to be justified, because of a lack of equilibrium between rotational and translational degrees of freedom in the free jet reactor. Under the conditions of our experiments, the rotational temperature of the bromides is ~80 K, whereas the translational temperature is ~10 K. However, both of these temperatures clearly are essential and have to be taken into account: the rotational angular momentum of the molecules is important for average orientation, and their relative velocity defines the collisional time and energy. Su[22] considered the efficiency of ion−dipolar molecule capture under various collisional energies (from thermal energy to energies of a few electron volts) and constant rotational temperature of the neutrals (300 K), but those conditions are quite different from ours. However, even based only on comparison with the ADO model, we can conclude that the measured rate coefficients have reasonable values.

The rate coefficients k_1 and k_4 for the atom-transfer reactions of the HBr^+ and DBr^+ ions with the parent molecules were observed to be very similar to those measured in our previous work, whereas the rate coefficients k_2 and k_5 for atom transfer between different isotopic species seemed to be slightly higher (~20%). A remarkable (~70%) isotope effect was observed only for the charge-transfer reactions between the Br^+ ions and the HBr and DBr molecules; this effect remains unexplained. The enthalpy of reaction, which is defined as the difference of the heats of formation at $T = 0$ K (see Table 1), is unlikely to be responsible for the effect, which was equally observed for all REMPI schemes. If the Br^+ ions were produced in photodissociation of the HBr^+ and DBr^+ ions, the variation of the photon energies for different REMPI schemes was much more than the enthalpy of reaction. The excess of energy could be converted to internal energy of the Br^+ ions (exciting the different ^3P_J ground fine structure states or even the ^1D excited state, lying 11 409 cm^{-1} higher) and/or their kinetic energy, that ultimately may change the enthalpy of reaction dramatically.

A second surprise is the relatively low value of the rate of the simple charge-transfer DBr^+/HBr reaction (up to a factor of $^1/_3$ of that of the atom-transfer channel). As verified by numerical simulation, the final ion fractions measured in the experiment were least sensitive to the rate coefficients k_3 and k_6. That led to lower accuracy of the rate coefficients, which was probably caused by the initial creation of both types of ions at the ionization point z_i. The room-temperature rate

coefficient k_6 (in units of 10^{-10} cm^3/s, ±20%) was measured by Xie and Zare[9] as 4.1, 1.4, 3.8, and 2.3 for the DBr^+ [$\Pi_{3/2}$, $v = 0$], [$\Pi_{3/2}$, $v = 1$], [$\Pi_{1/2}$, $v = 0$], and [$\Pi_{1/2}$, $v = 1$] ion states, respectively. These are a factor of 2−3 less than those measured presently at low temperatures. The difference is the same for the rate coefficient k_1 (see Table 1 and ref 3) and can be explained in the frame of the model of the ion−dipole interaction.

Green et al.[3] studied different channels of the reactions between the $H^{79}Br^+$ ions and $H^{79,81}Br/D^{79,81}Br$ molecules and found that the charge-transfer, proton-transfer, and hydrogen/deuterium-transfer channels amounted to 46%/50%, 32%/28%, and 21%/21%, respectively. In the present study, we cannot distinguish the products of proton and hydrogen (for HBr^+/HBr) or deuterium (for HBr^+/DBr) transfer reactions. However, we can estimate a portion of the charge-transfer channel in the HBr^+/DBr and DBr^+/HBr reactions, which is ∼20%−30%. This percentage is lower than those observed Green et al.[3] and is primarily caused by an increase of the proton/hydrogen/deuterium transfer rate at lower temperatures.

The only reactions that demonstrate dependence on the internal state of the ionic reactants or, more exactly, on vibrational excitation were reactions R1 and R4 (refer to Table 1). The difference in the rate coefficients is small (20%−40%), but it exceeds the experimental uncertainty. This tendency is observed for both reactions and for both spin−orbit states in every reaction, as well as in the work of Xie and Zare.[9] Thus, the favorable reactivity of ions in the ground vibrational state is statistically confirmed. A similar effect of rotational excitation has not been observed in our experiments. According to REMPI−LIF,[29] REMPI−PES, and zero-kinetic-energy−pulsed-field ionization (ZEKE−PFI)[30] studies, only a few rotational levels of the HBr^+ ion are populated about the *J*-value of the intermediate state selected. In most cases, we realized REMPI through the lowest rotational level of the intermediates, using the *R*(1) and *S*(0) rotational lines, populating a few of the lowest rotational levels of the ions. However, in several experiments, the higher lines—*R*(4), *R*(5), *S*(3), *S*(4)—were explored without any noticeable effect on the rate coefficients of the reactions studied. In most studies,[31−38] the effects of ion rotational excitation on ion−molecule reactions were either immeasurably small or <10% toward suppression of reactivity.[33,34] Yet, sometimes the effect of suppression was significantly stronger.[38,39] The effects of vibrational excitation of ions on reactivity has been observed to be ambiguous.[9,37,38,40−49] In some cases, the vibrational energy simply promotes overcoming an activation barrier for an endoergic reaction; in other cases, it is important in reaction dynamics and the competition of different reaction channels. Dependence of the rate coefficients on vibrational energy of ionic reactants could be explained, if we suppose that the reaction goes through a collisional complex formation. Green et al.[3] estimated that ∼28% of the HBr^+/DBr proceeded through a long-lived complex under thermal conditions. The fraction of the complex forming the channel would be expected to increase at lower temperatures and is possibly dominant under the near-10-K conditions realized in our experiments. An inverse vibrational dependence of the rate coefficients can result in a complex formation mechanism. Roughly, a complex produced from an ion in the ground vibrational state can decay to new products or return to original reactants, whereas a complex produced from a vibrationally excited ion has the additional channel of vibrational relaxation. Regardless of the mechanism that is responsible for the lower reactivity of the vibrationally excited HBr^+ and DBr^+ ions, this weak (∼20%−40%) effect has been observed for reactions R1 and R4 only and is not observed for the similar reactions R2 and R5.

VIII. Summary

The charge- and atom-transfer reactions between the HBr^+, DBr^+, and Br^+ ions and the HBr and DBr molecules have been studied under low-temperature conditions in a helium free jet. The HBr^+ [$^2\Pi_i$, v^+] and DBr^+ [$^2\Pi_i$, v^+] ions were prepared in selected spin−orbit ($i = {}^1/_2$ or ${}^3/_2$) and vibrational ($v^+ = 0$ or 1) states by (2+1) REMPI through the $f\,^3\Delta_2$ ($v = 0$), $f\,^3\Delta_2$ ($v = 1$), $F\,^1\Delta_2$ ($v = 0$), and $F\,^1\Delta_2$ ($v = 1$) Rydberg intermediates. Despite the resonance character of the ionization, a small, but finite, quantity of byproduct ions (Br^+ and $H(D)Br^+$) were created and observed in each ionization path. All ions (reactants and products) were measured by time-of-flight (TOF) mass spectrometry at some distance from the ionization point z_i. The kinetics of these ions, under a variety of [HBr] and [DBr] concentrations, has been used to derive the rate coefficients of all energetically permitted reactions. All highly exothermic reactions, including the Br^+/(HBr, DBr) charge transfer and (HBr^+, DBr^+)/(HBr, DBr) hydrogen/deuterium transfer, are observed to be fast (1.0×10^{-9}−2.7×10^{-9} cm/s, values of which are similar to the rate coefficients of the ion−polar molecule capture estimated in the context of the average dipole orientation (ADO) model. The low-temperature rate coefficient of the HBr^+($^2\Pi_{3/2}$, $v^+ = 0$)]/HBr hydrogen-transfer reaction exceeds its room-temperature value measured by Green et al.[3] by as much as a factor 2, whereas the rates of almost equi-energetic DBr^+/HBr and HBr^+/DBr charge-transfer reactions are more similar to those measured by Xie and Zare[9] for $T =$ 300 K. Only atom-transfer reactions between the same isotopic species demonstrate a weak negative dependence on vibrational excitation of the ions that can be explained if the reaction proceeds through a long-lived, complex forming mechanism. This work also demonstrates that multireaction processes can be successfully studied by a single spectroscopic technique, even for cases in which the reaction products are not all directly observed.

Acknowledgment. The authors gratefully acknowledge financial support of this work by the National Science Foundation, through Grant No. CHE-9984613, and by the Russian Foundation of Basic Research, through Grant No. 03-03-32316. We also thank the reviewers for useful comments and suggestions.

References and Notes

(1) Belikov, A. E.; Mullen, C.; Smith, M. A. *J. Chem. Phys.* **2001**, *114*, 6625.

(2) Belikov, A. E.; Smith, M. A. *Chem. Phys. Lett.* **2002**, *358*, 57.

(3) Green, R. J.; Xie, J.; Zare, R. N.; Viggiano, A. A.; Morris, R. A. *Chem. Phys. Lett.* **1997**, *277*, 1.

(4) Su, T.; Bowers, M. T. In *Gas-Phase Ion Chemistry*; Academic Press: New York, 1979; Vol. 1, Ch. 3, p 83.

(5) Dotan, I.; Lindinger, W. *J. Chem. Phys.* **1982**, *76*, 4972.

(6) Rebrion, C.; Rowe, B. R.; Marquette, J. B. *J. Chem. Phys.* **1989**, *91*, 6142.

(7) Smith, M. A. In *Unimolecular and Bimolecular Ion−Molecule Reaction Dynamics*; Ng, C. Y., Baer, M., Powis, I., Eds.; Wiley: New York, 1994; p 183.

(8) Belikov, A. E.; Kusnetsov, O. V.; Sharafutdinov, R. G. *J. Chem. Phys.* **1995**, *102*, 2792.

(9) Xie, J.; Zare, R. N. *J. Chem. Phys.* **1992**, *96*, 4293.

(10) Smith, M. A.; Hawley, M. In *Advances in Gas-Phase Ion Chemistry*; Adams, N. G., Babcock, L. M., Eds.; JAI Press: Greenwich, CT, 1992; p 167.

(11) Penno, M.; Holzwarth, A.; Weitzel, K.-M. *J. Phys. Chem. A* **1998**, *102*, 1927.

(12) Lias, S. G.; Bartmess, J. E.; Liebman, J. F.; Holmes, J. L.; Levin, R. D.; Mallard, W. G. *J. Phys. Chem. Ref. Data* **1988**, *17* (Suppl. 1), 1.
(13) Ashkenas, H.; Sherman, F. In *Rarefied Gas Dynamics: Proceedings of the 4th International Symposium on Rarefied Gas Dynamics*; Academic Press: New York, 1966; Vol. 2, p 84.
(14) Miller, D. R. In *Atom and Molecular Beam Methods*; Scoles, G., Ed.; Oxford University Press: New York, 1987.
(15) Miller, D. R.; Andres, R. P. In *Rarefied Gas Dynamics: Proceedings of the 5th International Symposium on Rarefied Gas Dynamics*; Academic Press: New York, 1969; Vol. 2, p 1385.
(16) Cattolica, R.; Gallagher, R. J.; Anderson, J. B.; Talbot, L. *AIAA J.* **1979**, *17*, 344.
(17) Tanaka, K.; Kato, T.; Koyano, I.; Takahashi, N.; Moriya, T.; Teshima, K. In *Rarefied Gas Dynamics: Proceedings of the 14th International Symposium on Rarefied Gas Dynamics*; Oguchi, H., Ed.; University of Tokyo Press: Tokyo, 1984; Vol. 2, p 751.
(18) Theard, L. P.; Hamill, W. H. *J. Am. Chem. Soc.* **1962**, *84*, 1134.
(19) Moran, T. F.; Hamill, W. H. *J. Chem. Phys.* **1963**, *39*, 1413.
(20) Su, T.; Bowers, M. T. *J. Chem. Phys.* **1974**, *60*, 4897.
(21) Su, T.; Chesnavich, W. J. *J. Chem. Phys.* **1982**, *76*, 5183.
(22) Su, T. *J. Chem. Phys.* **1985**, *82*, 2164.
(23) Su, T. *J. Chem. Phys.* **1988**, *89*, 5355.
(24) Clary, D. C. *Mol. Phys.* **1985**, *54*, 605.
(25) Clary, D. C.; Smith, D.; Adams, N. G. *Chem. Phys. Lett.* **1985**, *119*, 320.
(26) Rebrion, C. J.; Marquette, J. B.; Rowe, B. R.; Clary, D. C. *Chem. Phys. Lett.* **1988**, *143*, 130.
(27) Troe, J. *Chem. Phys. Lett.* **1985**, *122*, 425.
(28) Troe, J. *Adv. Chem. Phys.* **1992**, *82*, 485.
(29) Xie, J.; Zare, R. *Chem. Phys. Lett.* **1989**, *159*, 399.
(30) Wales, N. P. L.; Buma, W. J.; de Lange, C. A.; Lefebvre-Brion, H.; Wang, K.; McKoy, V. *J. Chem. Phys.* **1996**, *104*, 4911.
(31) Chupka, W. A.; Russel, M. E.; Refaey, K. *J. Chem. Phys.* **1968**, *48*, 1518.
(32) Liao, C. L.; Liao, C. X.; Ng, C. Y. *J. Chem. Phys.* **1984**, *81*, 5672.
(33) Gerlich, D.; Rox, T. *Z. Phys. D: At., Mol. Clusters* **1989**, *13*, 259.
(34) Anderson, S. L. *Adv. Chem. Phys.* **1992**, *82*, 177.
(35) Softley, T. P.; Mackenzie, S. R.; Merkt, F.; Rolland, D. *Adv. Chem. Phys.* **1997**, *101*, 667.
(36) Green, R. J.; Qian, J.; Kim, H.-T.; Anderson, S. L. *J. Chem. Phys.* **2000**, *113*, 3002.
(37) Viggiano, A. A.; Williams, S. In *Advances in Gas-Phase Ion Chemistry*; Adams, N. G., Babcock, L. M., Eds.; Academic Press: New York, 2001; p 85.
(38) Viggiano, A. A.; Morris, R. A. *J. Phys. Chem.* **1996**, *100*, 19227.
(39) Schlemmer, S.; Lescop, E.; von Richthofen, J.; Gerlich, D.; Smith, M. *J. Chem. Phys.* **2002**, *117*, 2068.
(40) Chupka, W. A.; Berkowitz, J.; Russel, M. E. In *VI International Congress on the Physics of Electronic and Atomic Collisions: Abstracts of Papers*; MIT Press: Cambridge, MA, 1969.
(41) Govers, T. R.; Guyon, P.-M. *Chem. Phys.* **1987**, *113*, 425.
(42) Liao, S. L.; Xu, R.; Flesch, G. D.; Baer, M.; Ng, C. Y. *J. Chem. Phys.* **1990**, *93*, 4818.
(43) Kato, S.; de Gouw, J. A.; Lin, C.-D.; Bierbaum, V. M.; Leone, S. R. *J. Chem. Phys.* **1996**, *105*, 5455.
(44) Morris, J. R.; Kim, G.; Barstis, T. L. O.; Mitra, R.; Jacobs, D. C. *J. Chem. Phys.* **1997**, *107*, 6448.
(45) Knoff, W. J.; Proch, D.; Kompa, K. L. *J. Chem. Phys.* **1999**, *110*, 9426.
(46) Chiu, Yu.; Pullins, S.; Levandier, D. J.; Dressler, R. A. *J. Chem. Phys.* **2000**, *112*, 10880.
(47) Dressler, R.; Chiu, Yu.; Levandier, D. J.; Ng, C. Y. *J. Chem. Phys.* **2000**, *113*, 8561.
(48) Chiu, Y.-H.; Fu, H.; Huang, J.-T.; Anderson, S. L. *J. Chem. Phys.* **1996**, *105*, 3089.
(49) Poutsma, J. C.; Everest, M. A.; Flad, J. E.; Zare, R. N. *Appl. Phys. B* **2000**, *71*, 623.